



Universiteit
Leiden
The Netherlands

Dislocations in stripes and lattice Dirac fermions

Mesaroš, A.

Citation

Mesaroš, A. (2010, October 6). *Dislocations in stripes and lattice Dirac fermions*. *Casimir PhD Series*. Retrieved from <https://hdl.handle.net/1887/16013>

Version: Corrected Publisher's Version

License: [Licence agreement concerning inclusion of doctoral thesis in the Institutional Repository of the University of Leiden](#)

Downloaded from: <https://hdl.handle.net/1887/16013>

Note: To cite this publication please use the final published version (if applicable).

CHAPTER 6

METALLIC STRIPES AND THE BOND-STRETCHING PHONON ANOMALY IN CUPRATES

6.1 Introduction

The phonon spectrum of the high- T_c superconducting cuprates is characterized by a peculiar anomaly: halfway the Brillouin zone the bond-stretching Cu—O vibration mode seems to suddenly dip down to a much lower frequency [226–228]. The line-width reaches its maximum at a wavevector somewhat shifted from the frequency-dip position, while it *narrows* at higher temperatures [229, 230]. In addition, the anomaly has a narrow intrinsic peak width as function of momentum transversal to the mode propagation direction [229, 230]. While the position of the dip is doping-independent, the softening amplitude changes with doping [228, 231] tracking roughly the “Yamada plot” [232]. This is hard to explain in a conventional fermiology framework, and interpretations invoking a coupling between the phonon and purely electronic collective modes of the stripes acquired credibility [233] by the recent demonstration that the anomaly is particularly pronounced in $\text{La}_{2-1/8}\text{Ba}_{1/8}\text{CuO}_4$ [228–230], a system with a well developed static stripe phase [96]. Initially, Kaneshita *et al.* [234] considered a crossing of the LO-phonon with the transversal ‘meandering’ stripe fluctuations [235] by computing the Gaussian fluctuations around the Hartree-Fock stripe ground state. This interpretation is however problematic: it was deduced [98] using the anisotropy of the spin-fluctuations that in the untwinned YBCO superconducting crystal the

phonon anomaly occurs for phonon-wavevectors parallel to the stripes, at a right angle as compared to the expectations for transversal stripe modes.

A well known problem with the Hartree-Fock stripes is that they are “insulating like” [93], while cuprate stripes are quite metallic. This supports the idea that they form an electronic liquid crystal of the smectic kind as introduced by Kivelson and coworkers [100, 236, 237] (see also Chapter 7). Here the transversal modes are frozen out by commensuration effects and instead the low energy physics is governed by on-stripe compressional fluctuations. As it was already noticed some time ago [238], the electronic polarizability associated with the on-stripe Luttinger-liquid like physics should be strongly enhanced at the on-stripe $2k_F$ wavevectors and this feature might well govern the phonon anomaly (see Fig. 6.1). This view is actually supported by numerous experimental and computational evidence. First of all, one-dimensional structure of the electron momentum distribution function is documented by ARPES measurements in non-superconducting $\text{La}_{1.28}\text{Nd}_{0.6}\text{Sr}_{0.12}\text{CuO}_4$ in the commensurate static stripe-phase at $1/8$ hole-doping [239]. Besides, the high resolution ARPES data [240] in high- T_c ($T_c = 40\text{K}$) $\text{La}_{1.85}\text{Sr}_{0.15}\text{CuO}_4$, followed by a more detailed data for Sr concentration x ranging from $x = 0.03$ to $x = 0.3$ [241], indicate a dual nature of the electronic spectrum, that contains one-dimensional straight segments in the momentum distribution of the spectral weight in the $(\pi, 0)$ and $(0, \pi)$ antinodal regions superimposed on the 2D-like spectral weight distribution in the nodal direction $[1, 1]$ predicted by LDA calculations. These straight segments in the Brillouin zone would be expected to occur from 1D stripes along $[1, 0]$ or/and $[0, 1]$ direction in the CuO plane. The momentum distribution function integrated over 30meV interval around the Fermi-level, according to [240], suggests two sets of constant energy contours defined by the $|k_x| = \pi/4$ and $|k_y| = \pi/4$ lines, which would be indeed expected for superposition of two perpendicularly oriented stripe domains with quarter-filled charge stripes [239]. The 1D-like spectral weight crosses the Fermi-level at about the optimal doping $x = 0.15$ in $\text{La}_{2-x}\text{Sr}_x\text{CuO}_4$ [241]. This same spectral weight is observed as a “flat-band” or as the extended van Hove singularities (VHS) below the Fermi-level [241, 242] in the underdoped high- T_c cuprates, that are characterized with a transition into the pseudo-gap state. From the LDA+U model computations [243] side, there is also a prediction of metallic stripes with $4a_0$ (a_0 is the lattice constant in CuO plane) periodicity in $\text{La}_{15/8}\text{Sr}_{1/8}\text{CuO}_4$ high- T_c compound. The calculations give the semi-flat pieces of the quasi 1D Fermi-surface due to small interstripe hybridization $t_\perp \approx 15$ meV. Besides, recent STM measurements [99] in the so-called electronic cluster glass state (ECG) of strongly underdoped Na-CCOC and Dy-Bi2212 cuprates have revealed ‘nanostripe domains’ with a short-range $4a_0$ interstripe periodicity (see also Chapter 7). In this relation we mention that, as will become clear from the derivations presented here, the stripe-induced LO-phonon softening effect considered in our work is independent of the length of the stripe segments as long as the latter are longer than e.g. $10 \div 20$ lattice constants in the CuO plane, such that quantum size gap in the electronic spectrum related

with unidirectional motion along the finite length segment is substantially below the optical phonon frequency $\sim 0.1\text{eV}$.

Here we analyze the phonon anomaly as associated with an array of Luttinger liquids embedded into a 2D optical phonon background. We employ two simplifying assumptions: (i) we use the free fermion charge susceptibility (Lindhardt function) instead of the fully interacting Luttinger liquid form, since the phonon anomaly appears to be in first instance sensitive only to the gross features of the 1D electron dynamics. (ii) More critical, we assume that at the energy of the anomaly $\omega_{LO} \sim 68\text{meV}$ the inter-stripe hopping $\propto t_{\perp}$, and interaction effects can be neglected. Our theory gives a number of straightforward a posteriori explanations of the experiment, as well as provides several important predictions that are within reach of experiment. The list of both the explanations (three) and predictions (four), that follow from our theory, is presented below in logically formed sequence. (a) The stripe alignment problem is solved by construction, thus explaining parallel to the stripes alignment [98] of the phonon-wavevectors of the phonon anomaly in the untwinned YBCO superconducting crystal. Besides, our theory gives the following important prediction: (b) the anomaly is now caused by the phonon crossing the ubiquitous continuum of 1D charge excitations centered at the intrastripe $2k_F$ (Fig. 6.1). At the phonon frequency ω this continuum has a momentum width $\Delta q \approx k_F\omega/v_c$ where v_c is the electronic charge velocity and this causes a 'double dip' structure in the phonon spectral function (Fig. 6.2), as in the transversal stripe mode scenario [234] (inset Fig. 6.2). However, the big difference with the prediction [234] is that in the 'smectic scenario' the phonon is completely (Landau) damped in the momentum region in between the dips: high resolution neutron scattering measurements should be able to resolve this. (c) Another prediction is that the characteristic momentum where the anomaly occurs is now determined by the intrastripe electron density and not by the interstripe distance, hence, the position of the anomaly should have a doping dependence that is radically different from what is expected for transversal modes (Fig. 6.3). (d) We find a natural explanation for the correlation between the amplitude of the softening strength as function of doping and the Yamada plot [231]. (e) We explain why the anomalous phonon linewidth $\Delta\omega$ decreases with increasing temperature (Fig.6.4). (f) We show that the form factors of the electron-phonon interaction [244] localize the phonon anomaly in 2D momentum space also in the direction perpendicular to the stripes (Fig. 6.4), thus explaining the corresponding experiment [229, 230]. (g) Counterintuitively, we predict that the transverse width should contract when temperature is raised.

6.2 Elastic model of the CuO layer in the stripe phase

We embed the array of parallel metallic stripes in the 2D phonon universe by considering a simplified propagator: it describes non-interacting electrons in Bloch

states on a periodic array of parallel lines in two dimensions, moving freely along these lines, but with vanishing inter-line overlap of the ‘Wannier’ functions:

$$G(\vec{r}, \vec{r}'; i\omega) = \frac{1}{N_k} \sum_{\vec{k}} \sum_{l, l'=0}^{N-1} \frac{e^{i\vec{k}(\vec{r}-\vec{r}') + iQ(l y - l' y')}}{i\omega - \epsilon(\vec{k})} \quad (6.1)$$

where \vec{r}, \vec{r}' span the the 1D Cu-centered stripes (lines) in real space; ω is the Matsubara frequency. We consider an orthorhombic CuO plane, with a (b) being the unit cell spacing along the x (y)-axis. The stripe metallic direction is along the x -axis and the stripe Umklapp momentum $Q = 2\pi/bN$ is along the y -axis, where N ($= 4$ at higher doping) is the number of unit cells in one inter-stripe (charge-density) period. The momentum \vec{k} spans N_k sites in the reduced orthorhombic Brillouin zone $0 < k_y < 2\pi/bN$; $0 < k_x < 2\pi/a$. The electron dispersion $\epsilon(\vec{k}) \approx \epsilon(k_x)$, ignoring inter-stripe t_\perp (see above).

A hole on site \vec{r} inside the stripe communicates with neighboring oxygens’ bond-stretching displacements $u_{\pm i}^{\vec{r}} \equiv u_i(\vec{r} \pm \vec{i}/2)$, $\vec{i} = \vec{a}, \vec{b}$ and we take the effective coupling between those and the Zhang-Rice singlets as introduced by Khaliullin and Horsch [244],

$$H_{e-ph} = g_0 \sum_{\vec{r}} (u_x^{\vec{r}} - u_{-x}^{\vec{r}} + u_y^{\vec{r}} - u_{-y}^{\vec{r}}) c_{\vec{r}}^\dagger c_{\vec{r}} \quad (6.2)$$

with $g_0 \approx 2eV/\text{\AA}$, using the standard estimates for the charge transfer energy and hoppings [245]. This is actually our main step: from this Hamiltonian and the 2D ‘striped’ electron propagator Eq. (6.1) it is straightforward to calculate the self-energy part of the dynamical matrix associated with the CuO plane:

$$\Lambda_{x,y}^{E\alpha,\beta}(\vec{q}, \omega) = \frac{\omega_0}{N_k} \Pi(q_x, \omega) \begin{pmatrix} s_x^2 & s_x s_y \\ s_x s_y & s_y^2 \end{pmatrix} \quad (6.3)$$

where ω_0 is bare phonon frequency, $s_x = \sin(q_x a/2)$, $s_y = \sin(q_y b/2)$, and $\alpha, \beta = 1, 2, 3$ enumerate ions in the in-plane Cu—O unit cell: this particular form of the electron-phonon form-factors follows immediately from the tight binding Hamiltonian Eq. (6.2), implying actually a substantial dependence on the momentum q_y perpendicular to the stripes. $\Pi(q_x, \omega)$ corresponds with the polarization propagator of the (in principle, interacting) on-stripe Luttinger liquid, depending on the momentum component q_x along the stripes, while its fermion lines are given by the propagator Eq.(6.1). The prefactor $1/N_k$ arises because in the $\langle G \times G \sim \Pi \rangle$ product only terms diagonal in stripe-index are retained in the approximation of ‘independent stripe Luttinger liquids’: there are N_k such terms, while $G \times G \propto 1/N_k^2$ according to Eq. (6.1).

This self-energy has to be added to the bare (undoped) ab -plane ionic 6×6 dynamic matrix $\Lambda_{i,j}^{I\alpha,\beta}(\vec{q}, \omega)$ of the orthorhombic planes, constructed to be in close

6.3 “Fingerprints” of 1D stripe polarization in the phonon anomaly 91

agreement with the experimental data [228] for the in-plane bond-stretching LO phonon modes in the undoped cuprates:

$$\Lambda_{i,j}^{I\alpha,\beta}(\vec{q}, \omega) \propto \quad (6.4)$$

$$\propto \begin{pmatrix} \gamma^2(F+G) & 0 & -\gamma F c_x & 0 & -\gamma G c_y & 0 \\ 0 & \gamma^2(F'+G') & 0 & -\gamma F' c_x & 0 & -\gamma G' c_y \\ -\gamma F c_x & 0 & F & 0 & 0 & 0 \\ 0 & -\gamma F' c_x & 0 & F' & 0 & 0 \\ -\gamma G c_y & 0 & 0 & 0 & G & 0 \\ 0 & -\gamma G' c_y & 0 & 0 & 0 & G' \end{pmatrix}$$

where $\gamma \equiv \sqrt{\frac{m_O}{m_{Cu}}}$, with m_O and m_{Cu} being respectively the oxygen and copper ionic masses; C_x and C_y are shorthand for $\cos(q_x a/2)$ and $\cos(q_y b/2)$, respectively. We use $F = 0.44$, $F' = 0.18$, $G = 0.17$ and $G' = 0.40$ in units of $\epsilon_F \approx \tilde{t}_{pd}/2 \sim 100 \text{ meV}$. Here F is Cu—O coupling constant along the bond a parallel to the x -axis, and is slightly bigger than G' , which is Cu—O coupling along the bond b parallel to the y -axis. The number of different constants (four) reflects assumed orthorhombic symmetry of the unit cell in the CuO plane. This matrix allows for two mid-bond oxygen atoms surrounding the Cu atom in the in-plane orthorhombic unit cell. We concentrate on the in-plane stretching modes, thus, the apical oxygen degrees of freedom are neglected.

The phonon spectra $\omega_\sigma(\vec{q})$ associated with polarizations $\vec{e}_{\vec{q},\sigma}^\alpha$ are obtained by the diagonalization of the total dynamic matrix [246]. This is done by solving the following dynamic matrix equation [246]:

$$\sum_{\beta,j} \left\{ \Lambda_{i,j}^{I\alpha,\beta}(\vec{q}, \omega) + \Lambda_{i,j}^{E\alpha,\beta}(\vec{q}, \omega) \right\} e_{j,\vec{q},\sigma}^\beta = \omega_\sigma^2(\vec{q}) e_{i,\vec{q},\sigma}^\alpha \quad (6.5)$$

From these solutions the phonon spectral functions given by the imaginary part of the phonon propagator $D(\vec{q}, \omega)$ are obtained. Notice that the Λ^E 's are in general complex quantities, with the effect that $\omega_\sigma(\vec{q})$ acquires an imaginary part representing the phonon damping.

6.3 “Fingerprints” of 1D stripe polarization in the phonon anomaly

We use for $\Pi(q_x, \omega)$ the well known 1D Lindhardt function [247],

$$\text{Re}\Pi(q, \omega) = -\frac{\omega_0 \xi}{4\pi q \tau} \int_0^\infty \ln \left| \frac{\Delta_+}{\Delta_-} \right| \cosh^{-2} \left(\frac{p^2 - 1}{2\tau} \right) p dp \quad (6.6)$$

$$\text{Im}\Pi(q, \omega) = \frac{\omega_0 \xi}{8} \left[\tanh \frac{\omega + 2(q-2)}{4\tau} + \tanh \frac{\omega - 2(q-2)}{4\tau} \right], \quad (6.7)$$

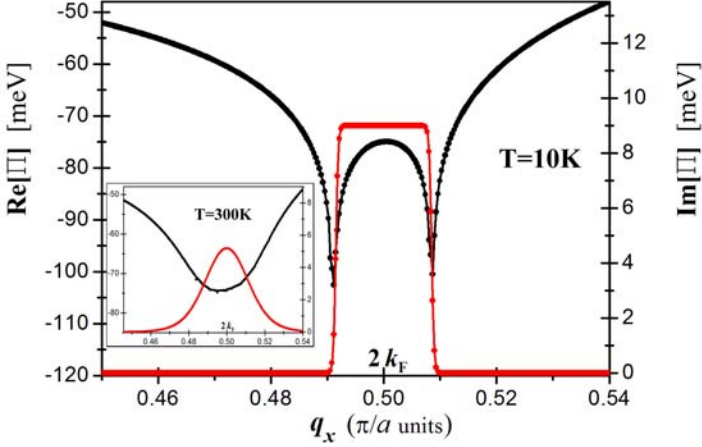


Figure 6.1: Real— (black line) and imaginary (red line) part of the on-stripe electronic phonon self-energy $\Pi(q_x, \omega)$ at $T = 10\text{K}$ at a fixed (phonon) frequency $\omega = 68\text{meV}$, as function of the momentum component q_x parallel to the stripes. We take for the dimensionless electron-phonon coupling a value representative for the cuprates: $\xi = 1.0$. In the inset the results are shown at a higher $T = 300\text{K}$.

where $\Delta_{\pm} = (2p \pm q)^2 q^2 - \omega^2$, all momenta and energies are measured in units of the Fermi-gas parameters k_F and $\epsilon_F \equiv k_F^2/2m \sim 0.1\text{eV}$, while $\tau = k_B T/\epsilon_F$ is a dimensionless temperature. The dimensionless electron-phonon coupling constant $\xi = g_0^2/K\epsilon_F \sim 1$ is representative for cuprates with $K \approx 25\text{eV}/\text{\AA}^2$ the lattice force constant [244].

6.3.1 Doping dependence of the phonon anomaly

The effect of this 1D polarizability on the phonons follows from the behavior of $\Pi(q_x, \omega)$ at the phonon-frequency $\omega = \omega_0$ as function of q_x (Fig. 1). The continuum of charge excitations in a 1D fermi-gas is the well known fan in the momentum-frequency plane, centered at $2k_F$ at $\omega = 0$ and bounded by $2k_F \pm \omega/v_F$ at finite frequency. For non-interacting electrons the spectral function ($\text{Im}\Pi$) is just the box of Fig. (6.1), while in the presence of interactions the spectral weight will pile up at the edges. Since Π is proportional to the phonon self-energy, the phonon spectral function, Fig. (6.2), indicates that the phonon dispersion is pushed downwards when it approaches the edges of the quasi 1D electron-hole continuum from either side, to broaden strongly when it enters the continuum. This is markedly different from the result based on a mode coupling between the phonon and a propagating mode as for instance discussed

6.3 “Fingerprints” of 1D stripe polarization in the phonon anomaly⁹³

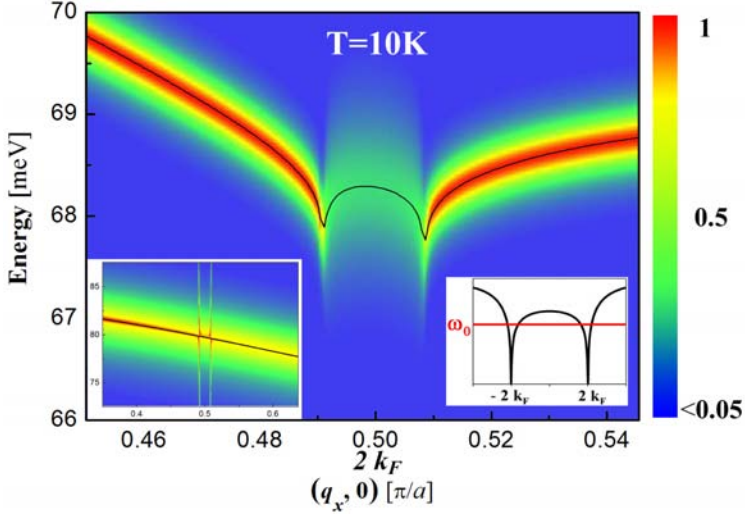


Figure 6.2: False color plot of the LO phonon spectral function *vs* momentum in the stripe direction and energy at low temperature (10K) for 1D $\epsilon_F \sim 0.1\text{eV}$ and the same parameters as in Fig. 6.1. Phonons couple merely to the 1D Fermi-gas like charge excitations of the metallic electron system confined in the stripes. Strong phonon damping in a momentum region ‘inside’ the anomaly is caused by the decay in the continuum of quasi 1D electron-hole excitations. Left inset: different behavior of the ‘standard’ mode coupling of the phonon with a propagating stripe collective mode (e.g., Ref. [234]). Right inset: the renormalized phonon dispersions determined by the crossing of the phonon frequency ω_0 and the real part of the 1D polarization propagator of Fig. 6.1 (see text).

by Kaneshita *et al.* [234] and shown in the inset of Fig. (6.2): in this case there is no phonon damping and the intensity is just distributed over the propagating modes subjected to an avoided level crossing. The bottomline is that the gross effect of the two scenarios is quite similar and to find out the difference higher resolution measurements are required.

A distinction between the effects of the transversal stripe modes and the internal 1D-like fermionic excitations on the phonon anomaly should also be revealed by the different doping dependence of the locus of the phonon anomaly in momentum space. The transversal fluctuations emerge at the stripe ordering wavevectors and these should follow the famous Yamada plot [232], correlating the stripe ordering wavevectors δ with doping x (Fig. 6.3), such that at low dopings the anomaly should live at a wavevector $q_a \sim 1/x$. On the other hand, dealing with the quasi 1D modes the locus of the anomaly is determined by the on-stripe hole density and according to the Yamada plot this stays constant (‘half-filled’) at $q_a = 2k_F = \pi/2a$ up to $x_c = 1/8$, while at higher dopings $x > x_c$

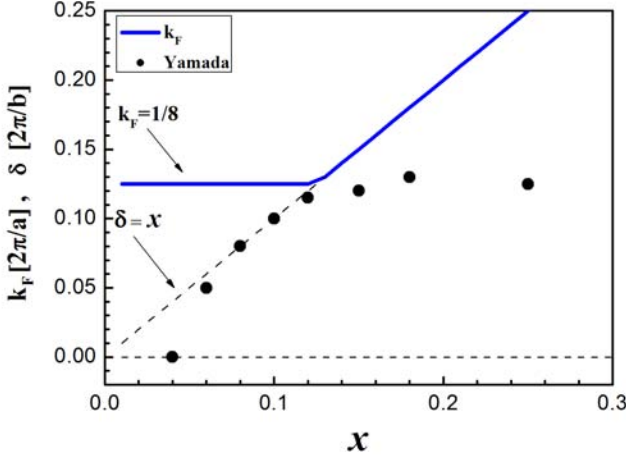


Figure 6.3: The qualitatively different doping dependences expected for the characteristic wavevector of the anomaly when transversal stripe model (1) or the intra-stripe quasi 1D electron excitations (2) are responsible. In case (1) the anomaly should follow the stripe-ordering incommensurate wavevector δ dependence on doping x : the famous “Yamada plot” [232] (black dots); (blue line) is for the softened phonon wavevector $q = 2k_F$, and black dots — for the softening strength in case (2).

it should follow $q_a = 2k_F \propto x$ because the on-stripe hole density is increasing (the blue line in Fig. 6.3). Experimentally the locus of the anomaly in k -space is conspicuously doping independent [228], actually arguing strongly against the transversal mode. It would be interesting to find out if the ‘center of mass’ of the anomaly does shift at higher dopings. Remarkably, the prefactor $1/N_k$ in the phonon self-energy Eq. (6.3) and, hence, the softening amplitude $\Delta\omega \propto \Pi/N_k$ depends on doping x roughly in the same way as given by the “Yamada plot” [232] (black dots in Fig. 6.3). This should be true for both the amplitude of the sharp feature around $q_a \sim 2k_F = \pi/2a$ (the double-dip in Fig. 6.2), and the amplitude of the “smooth” softening across the half Brillouin zone, which is caused by the momentum-dependent form-factors $s_{x,y} = \sin(q_x a/2), \sin(q_y b/2)$ in the 2×2 matrix multiplied by Π/N_k in Eq. (6.3). The latter fact may explain naturally why the amplitude A in the phenomenological function $0.5A \cos(q_x a) + B$ follows the “Yamada plot” as function of hole doping x (see Fig. 4 of [231]), as long as this function is used [231] to fit the smooth part of the measured bond-stretching phonon softening in $\text{La}_{2-x}\text{Sr}_x\text{CuO}_4$.

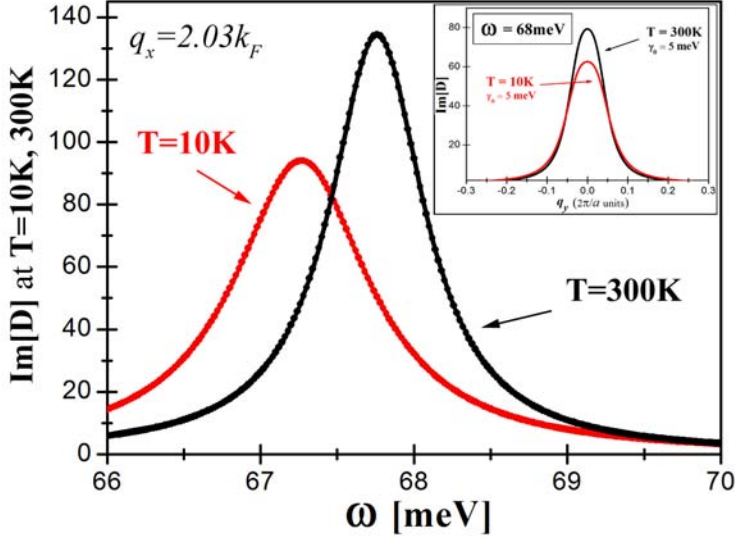


Figure 6.4: Calculated phonon spectral function $\text{Im}D(q_x, q_y = 0; \omega)$ dependence on frequency ω , using the same parameters as in Fig. 6.2, at different temperatures. A temperature narrowing is manifest (in accord with experiment [229]), accompanied by a phonon hardening at the ‘dips’ seen in Fig. 6.2. Inset: calculated $\text{Im}D(q_x, q_y; \omega)$ momentum dependence in the ‘transversal’ q_y direction perpendicular to the stripes, at fixed $q_x = 2k_F$ and $\omega = 68\text{meV}$. Counter intuitively, the anomaly even localizes further when temperature is raised.

6.3.2 Temperature and wave-vector dependence of the phonon anomaly

Our theory yields a rationale for the observed gross temperature dependence of the anomaly [229]. The rather counterintuitive narrowing of the frequency width with increasing temperature follows naturally from the temperature dependence of the 1D polarization propagator: $\text{Im}\Pi \propto \omega/T$ (Fig. 6.1). The effect of this change on the phonon spectral function is shown in Fig. (6.4): a substantial narrowing occurs at higher temperature. Moreover, right at the ‘dips’ a substantial phonon hardening occurs since the phonon positions at these momenta are most sensitive to the details of the real part of the self energy.

The phonon anomaly behavior in the ‘transversal’ q_y -direction (inset, Fig. 6.4) follows from our analysis of the expression for the phonon spectral function $\text{Im}D(q_x, q_y; \omega)$, showing a substantial q_y dependence close to the anomaly due to the form-factors in Eq. (6.3):

$$\text{Im}D(q_x, q_y; \omega) \approx \frac{\omega_0 \Delta_{q_x, q_y} \text{Im}\Pi_{q_x}}{4(\tilde{\omega}_{q_x, q_y} - \omega)^2 + \Delta_{q_x, q_y}^2 \text{Im}^2\Pi_{q_x}}, \quad (6.8)$$

where $\Delta_{q_x, q_y} \equiv s_{q_x}^2 + s_{q_y}^2$, and $\tilde{\omega}_{q_x, q_y} \approx \omega_0 + 0.5\Delta_{q_x, q_y} \text{Re}\Pi_{q_x}$ is the renormalized optical phonon mode frequency. The width of the Lorentzian with respect to q_y at $\omega = \tilde{\omega}_{q_x=2k_F, q_y=0}$ is: $\delta q_y \approx 2/a\sqrt{|\text{Im}\Pi/\text{Re}\Pi|} \sim 0.1 \times 2\pi/a$, assuming a flat bare mode dispersion. Given the ratio under the square root, the width δq_y decreases when the temperature is raised.

6.4 Conclusions

In summary, we have analyzed a minimal, (over)simplified model dealing with the Luttinger liquid-like excitations coming from the electrons confined in stripes interacting with optical lattice phonons. Our main new finding is that the gross features of the phonon anomaly as measured experimentally are consistent with the workings of a quasi 1D array of metallic intrastripe Luttinger liquids. Their fingerprints described above include binding of the anomalous phonon momentum to 1D intrastripe $2k_F$ wavevector and hence to its doping dependence; a Yamada plot behavior of the softening strength; a decrease with increasing temperature of the phonon line-width and of the spread of the anomaly in the transverse momentum; and finally, a double-dip structure of the bond-stretching phonon anomaly that should be observable at high enough resolutions.